Int. J. Heat Mass Transfer. Vol. 15, pp. 1745–1763. Pergamon Press 1972. Printed in Great Britain

ANODE HEAT TRANSFER FOR A FLOWING ARGON PLASMA AT ELEVATED ELECTRON TEMPERATURE†

TARIT K. BOSE

Jet Propulsion Laboratory, Pasadena, California, U.S.A.

(*Received* 14 *April* 1970 *and in revised form* 6 *October* 1970)

Abstract—Heat transfer from a pre-ionized gaseous plasma flowing over an anode surface at an elevated electron temperature in the presence of an electric field normal to the surface is investigated theoretically. A laminar boundary layer is considered in which only the velocity profile is locally similar and fluid properties are assumed to change uniformly in the gas flow direction. Results obtained by an approximation method show that for moderate current densities $|j_e| < 10^6$ A/m^2, the velocity and temperature distributions are insensitive to current. In addition, the effect of elevated electron temperature is negligible on convective heat transfer, but is significant for the overall heat transfer due to the enthalpy transport by current. Total heat flux to the anode is obtained by evaluating the Nusselt number and adding terms due to the potential drop in the sheath and the surface work function.

NOMENCLATURE

a, atoms;
b, outer edge of the free-fall region;
C, density-viscosity product ratio, $\rho\eta/_\infty\eta_\infty$;
c, thermal velocity [m/s];
D, diffusion coefficient [m^2/s];
D_{amb}, ambi-polar diffusion coefficient [m^2/s];
D_0, characteristic diameter [m];
e, elementary charge = $1{\cdot}602 \times 10^{-19}$ [as];
e, electrons;
E, internal energy [J/kg];
E'_f, externally applied electric field [V/m];
F, a function, equation (46);
f, reduced stream function = $\Psi/\sqrt{2s}$;
g_j, species mass density ratio, ρ_j/ρ;
g_j^*, g_i/g_{jo};
h, enthalpy [J/kg];
I_i, ionization potential [eV];
I_{mi}, ionization potential per unit mass ion [J/kg];
i, ions;
J, current function, equation (25);
j, current density [A/m^2];
j_e, electron current density [A/m^2];
K, constant, equation (35);
k, thermal conductivity coefficient [J/m°Ks];
k_S, Spitzer's thermal conductivity coefficient [J/m°Ks];
k_B, Boltzmann constant = $1{\cdot}38 \times 10^{-23}$ [J/°K];
L, characteristic length [m];
L_c, defined length, [m], equation (53);
M, mass of particle [kg];
m, mol mass of particle [kg/kmol];
m_R, mass rate of production [kg/m^{3}s];
N_1, N_2, dimensionless numbers, equations (27) and (31);
Nu, Nusselt number for $T_w \ll T_{ho}$, equation (30);
n, number density [m^{-3}];
$\dot{n}$, flux of particles [m^{-2}s^{-1}];

† This paper presents the results of one phase of research carried out in the Propulsion Research and Advanced Concepts Section of the Jet Propulsion Laboratory, California Institute of Technology, under Contract No. NAS 7-100, sponsored by the National Aeronautics and Space Administration.

Pr, Prandtl number;
p, pressure [bar];
Q, collision cross section [m^2];
$Q_{e,\text{chem}}$, reaction energy carried away by electrons [J/m^3s];
q, heat flux [J/m^2s];
q_R, radiative heat flux [J/m^2s];
R, reaction rate [$m^{-3}s^{-1}$];
R^*, universal gas constant = 8314 [J/kmol°K];
Re, Reynolds number;
r, radius [m];
r_0, radius of cross section of the body of revolution [m];
S_j, source terms, equations (23), (25) and (27);
S, Saha function, equation (45);
Sc, Schmidt number = $\rho D/\eta$;
s, transformed coordinate along body surface, equation (18);
T, temperature [°K];
T^*, T/T_0;
u, v, gas velocities in x, y directions, respectively [m/s];
U, characteristic velocity [m/s];
V, velocity vector [m/s];
x, y, distance along and normal to the body surface, respectively [m];
x_j, mol ratio;
Z, partition function;
α, correction factor, equation (50);
α_i, ionization fraction;
β, velocity gradient parameter, equation (21);
δ, Kronek's delta, equation (4);
δ^*, displacement thickness, equation (36);
δ_m, momentum thickness, equation (37);
δ_c, collision loss factor, equation (5);
η, dynamic viscosity [kg/ms];
ϕ_w, work function [V];
φ, potential drop [V];
φ_A, anode potential with respect to plasma [V];
Γ, collision frequency [$m^{-3}s^{-1}$];
λ, mean free path [m];
λ_e, mean free path of the electrons [m];
λ_{De}, Debye shielding distance [m];
μ_e, mobility coefficient of electrons [m^2/Vs];
ρ, density [kg/m^3];
σ, electrical conductivity [A/Vm];
θ, temperature ratio = T_e/T_h;
τ, stress term, equation (4);
ω, velocity gradient, equation (4);
ξ, non-dimensional coordinate normal to the body surface;
Ψ, stream function, equation (17);
∇, vector operator.

Subscripts and superscripts

a, atom;
b, condition at one mean free path from body surface;
e, electrons;
h, heavy particles;
i, ions;
j, any species;
0, condition at a reference point;
r, s, coordinate directions;
s, sheath condition;
s, ξ, derivatives with respect to transformed coordinates;
w, wall condition;
∞, condition at edge of the boundary layer;
$*$, non-dimensionalized properties.

I. INTRODUCTION

INTENSE heat flux to electrode surfaces, especially to the anode, is a critical factor that must be taken into account to prevent failure of plasma propulsion and power generation devices. A method of predicting the heat flux to anode surfaces is presented in which a laminar boundary-layer flow is considered with an electric field applied normal to the surface. Although the coupled non-linear system of differential equations is simplified by the laminar boundary layer approach, a strictly locally similar solution is possible only in very special cases. Even for

the case of chemical and thermal equilibrium ($T_e = T_h$), a locally similar solution is possible only, for example, if the current density $|j_e| \propto x^{-0.5}$, $j_x = 0$, or if $j_y = j_x = 0$. Therefore, it is proposed that the velocity profile alone is locally similar and that other terms representing non-similar behavior of the fluid properties are constant over the boundary-layer thickness but vary along the gas flow direction.

To solve the equations, more information of the thermophysical properties for two-temperature plasmas is required than is presently available. Hence, the composition of a plasma in chemical equilibrium is computed by the method of Kerrebrock [1] by replacing the temperature in the Saha equation by the electron temperature. Since the heavy particles appear almost static to the fast-moving electrons, it is believed reasonable to use the electron temperature to compute collision cross sections and frequency for collisions of electrons with heavy particles. Details of the computations for the thermophysical and transport properties are given in the Appendix.

Investigators who have studied related boundary-layer problems, but without applied fields, include Hayes [2] and other authors [3, 4] who attempted a non-similar solution of the boundary-layer equations by introducing the concept of growth of characteristic boundary-layer thicknesses and tried matching locally similar profiles for these. Hayes' analysis contains non-similar terms, but no source terms. In addition, he does not have the strongly interacting term which includes the energy exchange between the electrons and the heavy particles. Therefore, the solution of the differential equations converges more rapidly than in the present case. Though Sherman and Reshotko's analysis [4] represents the first step to solve the boundary-layer equations for a gas plasma at an elevated electron temperature, the solution must be started at a place where a complete profile is known. They present a numerical example of a magnetohydrodynamic channel in which the initial profiles are assumed to be at thermal equilibrium at an insulator section. Other differences between the present analysis and that of Hayes, and that of Sherman and Reshotko are that the present analysis contains source terms due to joule heating, and a local similar solution with given boundary conditions is assumed and does not require knowledge of the initial temperature profiles upstream. Furthermore, emphasis is placed on the heat transfer. The present analysis is readily suitable for use with several configurations. In addition to flow between parallel electrodes, for example, it can also be used for a hemispherical anode for which the stagnation point heat transfer, as well as the heat-transfer distribution, may be computed.

Several studies of heat transfer for an equilibrium plasma are given in the literature [5–10]; and formulation of the differential equation for a two-temperature plasma is available [4, 11, 12], but the heat-transfer relation for the latter case is not given. A simple anode heat transfer model was proposed by Shih *et al.* [13, 14] to empirically explain their experimental results in which the contribution of the electric current to the anode heat flux is separated from other heat-transfer mechanisms, and the overall contribution of the electric current to the anode heat flux is expressed as the sum of three individual contributions, i.e. the anode fall, the work function of the anode material, and the enthalpy carried by the electron current. This is also shown theoretically in the present analysis.

Several applications are shown in Fig. 1 in which heat-transfer relations from a gas plasma with electrons at elevated electron temperature to the cold anode wall are needed. In case of a current flow, a pre-ionized gas of sufficient electrical conductivity must flow over the body surface to have a finite potential drop between the free-stream and the body surface. A general relation expressed in terms of the Nusselt number, which is a function of the gradients of the temperatures and is applicable for each of the different physical situations shown in Fig. 1, is obtained and applied to special cases of

parallel flat-plate and axisymmetric stagnation-point boundary layers. A numerical solution for a specific gas, however, requires knowledge of the thermophysical properties. Methods are given to compute these properties, and the values are computed for the special case of an argon plasma. Thus, an approximate solution of the Nusselt number for an argon plasma is obtained by using a series polynomial equation for each differential equation and by computing the coefficients from given boundary conditions.

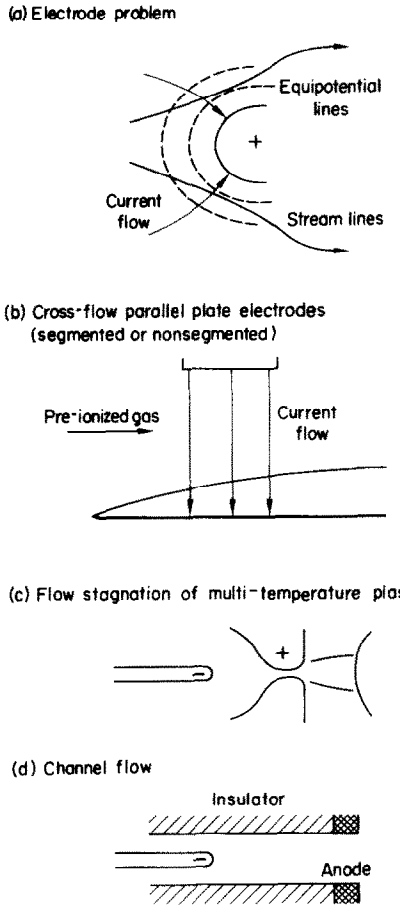

FIG 1. Applications for multi-temperature flow analysis.

II. ANALYSIS

A. *Assumptions*

The physical model for the anode heat flux is shown in Fig. 2. Since the anode is at a positive potential with respect to the plasma and the anode potential is believed to be "shielded" within a small distance, the ion current is considered to be negligibly small. From earlier computations for a singly ionized argon plasma in the pressure range 10^{-2}–10^{+2} bars (1 atm = 1·013 bar) [15], the mean free path of the electrons λ_e is 1–2 orders of magnitude larger than the Debye shielding distance λ_{De}, and the boundary-layer thickness λ_{BL} can be many orders of magnitude larger than λ_e. Thus, these conditions are also considered to exist in this analysis.

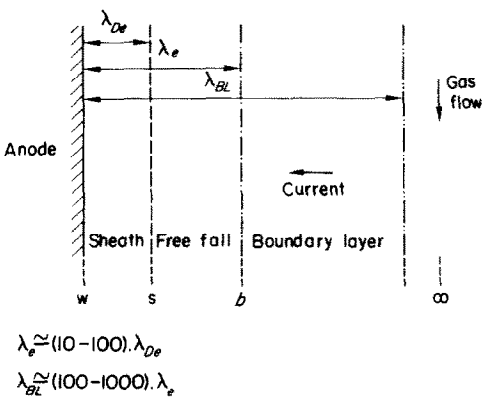

FIG. 2. Physical model for anode heat flux.

The underlying assumptions for the analysis are as follows:

(1) Steady, laminar, and continuum flow is outside b (Fig. 2). A free-fall region for electrons exists adjacent to the wall; the potential applied externally on the wall is assumed to be "shielded" within a distance on the order of λ_{De} (no large electrical field outside this region), which is designated as the sheath.

(2) The heavy particle temperature at b is equal to the temperature at the wall, $T_{hb} = T_w$.

(3) The radiation pressure is neglected; the radiative heat flux must be computed separately.
(4) There is no externally applied magnetic field, and the induced magnetic field is negligibly small.
(5) The current is carried mainly by the electrons.
(6) The plasma is quasi-neutral, i.e. $g_i = g_e m_h/m_e$ where $g_j = \rho_j/\rho$, $j = i, e$ for ions and electrons, respectively, and ρ = mass density.
(7) The kinetic energy of the gas is small in comparison to the total energy content.
(8) The pressure gradient and viscous terms are neglected in the energy equations but are retained in the momentum equation.
(9) The thermal diffusion and diffusion thermoeffects are neglected.

In addition to these assumptions, it is evident that for a current flow, the gas should be sufficiently pre-ionized.

B. *General equations*

With these assumptions, the equations describing the flow [12] can be written as follows:

(1) *Continuity of electrons.*

$$\rho V \cdot \nabla g_e - \nabla \cdot (\rho D_{\text{amb}} \nabla g_e) = m_{Re}, \text{ kg}_e/\text{m}^3\text{s}. \tag{1}$$

(2) *Continuity.*

$$\nabla \cdot (\rho V) = 0, \text{ kg/m}^3\text{s}. \tag{2}$$

(3) *Motion.*

$$\rho / V^r \nabla) \cdot V^s = \nabla \cdot \tau^{rs}, \text{ N/m}^3 \tag{3}$$

where

$$\tau^{rs} = \left[-p - \frac{2}{3} \eta \nabla \cdot V \right] \delta^{rs} + \eta \omega^{rs} \tag{4}$$

$$\delta^{rs} = 0, \delta^{rr} = 1$$

$$\omega^{rs} = \frac{\partial V^r}{\partial x^s} + \frac{\partial V^s}{\partial x^r}.$$

(4) *Electron energy*

$$\frac{3}{2}\frac{R^*}{m_e} \rho V \cdot \nabla (g_e T_e) = \frac{3}{2}\frac{R^*}{m_e} \nabla \cdot (\rho D_{\text{amb}} T_e \nabla g_e) + \nabla \cdot (k_e \nabla T_e) + Q_{e,\text{chem}} - \frac{3}{2}\frac{k_B}{e} \nabla \cdot (j_e T_e) + j_e \cdot E'_f - \frac{3 m_e}{m_h} k_B (T_e - T_h) \Gamma_{eh} \delta_c, \text{ J/m}^3\text{s}. \tag{5}$$

(5) *Heavy particles energy*

$$\frac{3}{2}\frac{R^*}{m_h} \rho V \cdot \nabla T_h + \rho I_{mi} \frac{m_h}{m_e} V \cdot \nabla g_e = + \nabla \cdot \left(\rho D_{\text{amb}} I_{mi} \frac{m_h}{m_e} \nabla g_e \right) + \nabla \cdot (k_h \nabla T_h) - Q_{e,\text{chem}} + \frac{3 m_e}{m_h} k_B (T_e - T_h) \Gamma_{eh} \delta_c \text{ J/m}^3\text{s}. \tag{6}$$

(6) *Global energy.*

$$\rho V \cdot \nabla h = \nabla \cdot (k_h \nabla T_h) + \nabla \cdot (k_e \nabla T_e) + \nabla \cdot \left(\rho D_{\text{amb}} I_{mi} \frac{m_h}{m_e} \nabla g_e \right) + \frac{5}{2}\frac{R^*}{m_e} \nabla \cdot (\rho D_{\text{amb}} T_e \nabla g_e) - \frac{5}{2}\frac{k_B}{e} \nabla \cdot (j_e T_e) + j_e \cdot E'_f. \tag{7}$$

(7) *Anode heat flux*

$$q_{\text{anode}} = q_b - j_e \cdot (\varphi_A + \phi_w) + q_R \tag{8}$$

where

$$q_b = -k_h \nabla T_h - k_e \nabla T_e - \rho D_{\text{amb}} \left(I_{mi} \frac{m_h}{m_e} + \frac{5}{2}\frac{R^*}{m_e} T_e \right) \nabla_{g_e} + \frac{5}{2}\frac{k_B}{e} j_e T_e. \tag{9}$$

An explanation is in order for an apparent discrepancy in the term representing the energy transport due to mass transport by diffusion in the global and species energy equations. This term in the species energy equations has a factor $\frac{3}{2}$; whereas, in the global equation the factor is $\frac{5}{2}$. By adding the species energy equations to form the global equation, the work done by the

diffusing particles against the stress tensor given in equation (4) is added to make this term $\Sigma\rho_j V'_j h_j$, which results in the factor $\frac{5}{2}$ instead of yielding the term $\Sigma\rho_j V'_j E_j$. This is also given by Hirschfelder [16].

An estimate of the temperature difference between the electrons and the heavy particles is possible by writing equation (5) for a current carrying volume element at uniform temperature [17] and neglecting chemical reaction:

$$j_e \cdot E'_f = en_e\mu_e E'^2_f = \frac{3m_e}{m_h} k_B(T_e - T_h)\Gamma_{eh} \approx \frac{3m_e}{m_h} k_B(T_e - T_h) n_e n_a c_e Q_{ae}$$

and by rearranging

$$T_e - T_h = \frac{e\mu_e E'^2_f}{3\left(\frac{m_e}{m_h}\right) k_B n_a c_e Q_{ae}}. \tag{10}$$

From equation (10) it appears that the temperature difference between the electrons and the heavy particles is independent of n_e. This is not the case since the electric field used in equation (10) is obtained from the relation $E'_f = j_e/(en_e\mu_e)$. Referring to equation (28), near the free-fall edge, n_e is very small for a current density $|j_e| < 10^6$ A/m^2. Consequently, E'_f becomes large and Γ_{eh} small in comparison to the values in the free stream. Thus, it is shown that the temperature of the current carrying electrons can deviate considerably from the temperature of the heavy particles. For the no-current case, however, $T_e \approx T_h$. Also, for small current density, Gray [18] estimated that for boundary layers at $p \leqslant 1$ bar, the electron temperature of the current carrying electrons at the sheath edge is approximately equal to that in the free stream.

C. *Boundary-layer equations*

The boundary-layer equations for a laminar, two-temperature plasma in the presence of an electric field perpendicular to the solid wall, as obtained by simplifying the general equations, are as follows:

(1) *Continuity of electrons.*

$$\rho u r_0^k \frac{\partial g_e}{\partial x} + \rho v r_0^k \frac{\partial g_e}{\partial y} - \frac{\partial}{\partial y}\left(\rho D_{\text{amb}} r_0^k \frac{\partial g_e}{\partial y}\right) = m_{Re} r_0^k \tag{11}$$

where

r_0 = radius of cross section of the body of revolution

$k = 0, 1$ for planar, axisymmetric bodies, respectively.

(2) *Continuity.*

$$\frac{\partial}{\partial x}(\rho u r_0^k) + \frac{\partial}{\partial y}(\rho v r_0^k) = 0. \tag{12}$$

(3) *Momentum.*

$$\rho u \frac{\partial u}{\partial x} + \rho v \frac{\partial u}{\partial y} = \rho_\infty U_\infty \frac{\partial U_\infty}{\partial x} + \frac{\partial}{\partial y}\left(\eta \frac{\partial u}{\partial y}\right). \tag{13}$$

(4) *Electron energy.*

$$\frac{3}{2}\frac{R^*}{m_e}\left[\rho u \frac{\partial}{\partial x}(g_e T_e) + \rho v \frac{\partial}{\partial y}(g_e T_e)\right] = \frac{3}{2}\frac{R^*}{m_e}\frac{\partial}{\partial y}\left(\rho D_{\text{amb}} T_e \frac{\partial g_e}{\partial y}\right) + \frac{\partial}{\partial y} k_e \frac{\partial T_e}{\partial y} + \frac{j_e^2}{\sigma} + Q_{e,\text{chem}} - \frac{3}{2}\frac{k_B}{e}\frac{\partial}{\partial y}(j_e T_e) - \frac{3m_e}{m_h} k_B(T_e - T_h)\Gamma_{eh}\delta_c. \tag{14}$$

(5) *Heavy particles energy.*

$$\frac{3}{2}\frac{R^*}{m_h}\left[\rho u \frac{\partial T_h}{\partial x} + \rho v \frac{\partial T_h}{\partial y}\right] + I_{mi}\frac{m_h}{m_e}\left[\rho u \frac{\partial g_e}{\partial x} + \rho v \frac{\partial g_e}{\partial y}\right] = \frac{\partial}{\partial y}\left[\rho D_{\text{amb}} I_{mi} \frac{m_h}{m_e}\frac{\partial g_e}{\partial y}\right] - Q_{e,\text{chem}} + \frac{\partial}{\partial y} k_h \frac{\partial T_h}{\partial y} + \frac{3m_e}{m_h} k_B(T_e - T_h)\Gamma_{eh}\delta_c. \tag{15}$$

(6) *Heat flux at* b.

$$q_b = k_h \frac{dT_h}{dy} - k_e \frac{dT_e}{dy} - \rho D_{amb} \left[I_{mi} \frac{m_h}{m_e} + \frac{5}{2} \frac{R^*}{m_e} T_e \right] \frac{dg_e}{dy} + \frac{5}{2} \frac{k_B}{e} (j_e T_e). \quad (16)$$

The overall continuity equation is automatically satisfied by introducing the stream function Ψ, which is defined as usual by the following relations:

$$\rho u r_0^k = \frac{\partial \Psi}{\partial y}, \quad \rho v r_0^k = -\frac{\partial \Psi}{\partial x}. \quad (17)$$

By introducing a transformation introduced by Lees [19], equations (11) to (16) are transformed from the x, y into the s, ξ coordinate system. The transformation relations in both coordinate systems are as follows:

$$s = \int_0^x \rho_\infty \eta_\infty U_\infty r_0^{2k} \, dx, \quad x = \int_0^s (\rho_\infty \eta_\infty U_\infty r_0^{2k})^{-1} \, ds \quad (18)$$

$$\xi = \frac{\rho_\infty U_\infty}{\sqrt{2s}} \int_0^y r_0^k \frac{\rho}{\rho_\infty} \, dy, \quad y = \frac{\sqrt{2s}}{\rho_\infty U_\infty} \int_0^\xi \frac{\rho_\infty}{\rho r_0^k} \, d\xi. \quad (19)$$

The terms T_e, T_h and g_e are made dimensionless (*) by dividing them by their respective values outside the boundary layers at a reference point with index 0, which for the planar case is at $x = 0$, and for axisymmetric bodies is just on the axis of the body.

Let $\Psi(s, \xi) = \sqrt{2s} f(s, \xi)$; then, equations (11)–(15) are transformed into s, ξ coordinate, where the subscripts s, ξ denote differentiation with respect to the respective coordinates, as follows:

(1) *Momentum.*

$$f f_{\xi\xi} + (C f_{\xi\xi})_\xi + \beta \left[\frac{\rho_\infty}{\rho} - f_\xi^2 \right] = 2s(f_\xi f_{\xi s} - f_s f_{\xi\xi}) \quad (20)$$

where

$$\beta = \frac{2s}{U_\infty} \frac{dU_\infty}{ds}, \quad C = \frac{\rho \eta}{\rho_\infty \eta_\infty}. \quad (21)$$

(2) *Continuity of electrons.*

$$f g_{e\xi}^* + (CSc g_{e\xi}^*)_\xi + 2s S_1 = 2s(f_\xi g_{es}^* - f_s g_{e\xi}^*) \quad (22)$$

where

$$S_1 = \frac{m_{Re}}{\rho \rho_\infty \eta_\infty U_\infty^2 r_0^{2k} g_{e0}}, \quad Sc = \frac{\rho D_{amb}}{\eta}. \quad (23)$$

(3) *Electron energy.*

$$f(g_e^* T_e^*)_\xi + \left[\left(\frac{C}{Pr_e} \right) T_{e\xi}^* \right]_\xi + (CSc T_e^* g_{e\xi}^*)_\xi - J(s) T_{e\xi}^* + 2s S_2 = 2s[f_\xi (g_e^* T_e^*)_s - f_s (g_e^* T_e^*)_\xi] \quad (24)$$

where

$$\left. \begin{aligned} S_2 &= \frac{2}{3} \frac{m_e}{R^*} \cdot \frac{1}{\rho \rho_\infty \eta_\infty U_\infty^2 r_0^{2k} g_{e0} T_{e0}} \left[\frac{j_e^2}{\sigma} - \frac{3 m_e}{m_h} k_B \delta_c (T_e - T_h) \Gamma_{eh} + Q_{e,\,chem} \right] \\ Pr_e &= \frac{3}{2} \frac{R^* g_{e0} \eta}{m_e k_e}, \\ J(s) &= j_e \sqrt{2s} \cdot \frac{k_B}{e} \frac{m_e}{R^* \rho_\infty \eta_\infty U_\infty r_0^k g_{e0}} \end{aligned} \right\}. \quad (25)$$

(4) *Heavy particles energy.*

$$f T_{h\xi}^* + N_1 (CSc g_{e\xi}^*)_\xi + N_1 f g_{e\xi}^* + \left[\left(\frac{C}{Pr_h} \right) T_{h\xi}^* \right]_\xi + 2s S_3 = 2s(f T_{hs}^* - f_s T_{h\xi}^*) + N_1 \cdot 2s(f_\xi g_{es}^* - f_s g_{e\xi}^*) \quad (26)$$

where

$$N_1 = \frac{2}{3} \frac{m_h^2 I_{mi} g_{e0}}{R^* T_{h0} m_e}, \quad Pr_h = \frac{3}{2} \frac{R^* \eta}{m_h k_h}$$

$$S_3 = \frac{2}{3} \frac{m_h}{R^*} \frac{1}{\rho \rho \eta U r_0^{2k} T_{h0}} \left[\frac{3 m_e}{m_h} k_B \delta_c (T_e - T_h) \Gamma_{eh} - Q_{e,\,chem} \right]. \quad (27)$$

One of the assumptions is that the applied potential at the anode is shielded within a short distance of the surface, that is, of the order of the

Debye shielding distance. Thus, for a current flow to the wall, a concentration gradient of the charged particles must be established at the sheath edge which is assumed to occur at the free-fall edge. By neglecting the ion currents, the following relation can be derived for current flow at the wall:

$$j_e = e(\dot{n}_{ew} - \dot{n}_{iw}) = -en_{eb}\left(\frac{k_B T_e}{2\pi M_e}\right)^{0.5} + en_{ib}\left(\frac{k_B T_h}{2\pi M_h}\right)^{0.5} \exp(-e\varphi_A/k_B T_h) \approx -en_{eb}\left(\frac{k_B T_e}{2\pi M_e}\right)^{0.5} \quad (28)$$

which can be transformed and rewritten into

$$g^*_{eb} = -j_e \frac{k_B}{e}\frac{m_e}{R^*}\left(\frac{2\pi M_e}{k_B T_{eb}}\right)^{0.5} \frac{1}{\rho_b g_{e0}}. \quad (28a)$$

Equation (28a) is used to compute the concentration of the electrons at b, the free-fall edge. The value of g^*_{eb} for argon at a current density $j_e = -10^6$ A/m^2 at a pressure of 1 bar and an electron temperature of 10000°K is about 10^{-7}. T_{eb} was taken equal to the free stream value as in Section III. For these conditions, there is a negligible contribution from the electrons to the thermal conductivity coefficient at the free-fall edge. The contribution of the electrons to the thermal conductivity coefficient k_e is computed with the help of Fay's mixing rule [20] using the value of k'_e for "pure" electrons. The value $k_e = 0(x_e k'_e)$, which is negligibly small near the free-fall edge because $x_e = n_e/\Sigma n_j$ is very small.

If no current flows, a negative potential develops on the wall, and the electron and ion fluxes at the free-fall edge are equal. For this special case only, it is, therefore, reasonable to assume that at b the normalized electron density gradient $g^*_{e\xi} = 0$. From equations (28) and (10), it can be shown that for the no current case ($E'_f = 0$), $T^*_{eb} \approx T^*_{hb}$. Sherman and Reshotko [4] include an additional equation from the energy conservation principle for the electrons at b to obtain a relation for T^*_{eb}. They obtained for an insulated wall the result $T^*_{eb} < T^*_{hb}$. This additional equation was abandoned in the present case on the grounds that, for small g^*_{eb} it is difficult to write at b an energy conservation relation for the electrons with any given accuracy. Because of some uncertainties in the value of T^*_{eb}, it is believed that at b, $T^*_{e\xi\xi} = 0$ is a better approximation than either $T^*_{eb} = T^*_{hb}$ or $T^*_{eb} = T^*_{e\infty}$. However, a consequence of using $T^*_{e\xi\xi} = 0$ for argon at low current density is that $T^*_{eb} = T^*_{e\infty}$, as is shown in Section III. The second derivative of the temperature at the free-fall edge (here, the second derivative of the electron temperature) equal to zero merely points out that at the free-fall edge, there is no heat source.

If there is no suction or blowing through the wall, the reduced stream function $f = \Psi/\sqrt{2s}$, evaluated at the wall, is of course zero. From the considerations above, the boundary conditions are:

$$\text{at } \xi \to 0: f = f_w = 0,\ f_{\xi b} = 0,\ T^*_{e\xi\xi b} = 0,\ g^*_e = g^*_{eb},\ T^*_h = T^*_{hw}$$

$$\text{at } \xi \to \infty: f_{\xi\infty} = 1,\ T^*_e = T^*_{e\infty},\ g^*_e = g^*_{e\infty},\ T^*_h = T^*_{h\infty}. \quad (29)$$

For the reduced stream function f and the temperature of the heavy particles T_h, the boundary conditions at the wall are generally known, although in the present analysis the values of these quantities are prescribed at the free-fall edge b, whereas T_e and g_e must be evaluated at the free-fall edge or, more precisely, at the sheath edge. As indicated in Fig. 2, however, these regions are considered to lie well within the boundary layer and are very close to the wall. Hence, for practical purposes the conditions stated in this region are interpreted as being either at the wall or in the vicinity of the wall, and are taken to be at the same location when introduced into the equations.

D. *Heat transfer*

By non-dimensionalizing equation (16) and transforming into the s, ξ plane, a characteristic

heat-transfer number ($q_b L/k_{hb}T_{h0}$) is found. Because of the similarity between this number and the usual definition of the Nusselt number for $T_w \ll T_{h0}$, this will also henceforth be referred to as the Nusselt number.

At the anode, the general relation for the Nusselt number may be written as

$$Nu_L = \frac{-q_b L}{k_{hb}T_{h0}} = \frac{1}{\sqrt{2}}\left(\frac{\rho_b}{\rho_\infty}\right)\sqrt{(Re_L)}\left[T^*_{h\xi b} + \frac{k_e}{k_h}\theta_0 T^*_{e\xi b} + N_1\left(\frac{Sc}{Pr_h}\right)_b g^*_{e\xi b} + \frac{5}{3}N_{2b}Sc_b\theta_0 T^*_{eb}g^*_{e\xi b} - \frac{5}{3}\frac{J\theta_0 N_{2b}}{C_b}\right] \quad (30)$$

where

$$Re_L = \frac{\rho_\infty^2 U_\infty^2 r_0^{2k} L^2}{s},\quad N_{2b} = \frac{3R^* g_{e0}\eta_b}{2m_e k_{hb}},\quad \theta_0 = \frac{T_{e0}}{T_{h0}}. \quad (31)$$

L = a characteristic length which for a flat plate is the distance from the leading edge, and for an axisymmetric body, like a sphere, a cylinder, etc., this length is the diameter.

The terms N_1 and N_2 represent the release of ionization energy by recombination and transportation of energy by diffusing electrons, respectively. In general, the second term in the bracket in equation (30), representing heat conduction by the electrons, is much smaller than the other terms because of the small electron mol ratio x_e and the small gradient of the electron temperature $T_{e\xi}$ near the wall and, therefore, can be neglected. With this limitation, the Nusselt number for a planar plate is

$$Nu_x = \frac{-q_b x}{k_{hb}T_{h0}} = \frac{1}{\sqrt{2}}\left(\frac{\rho_b}{\rho_\infty}\right)\sqrt{(Re_x)}\left[T^*_{h\xi b} + N_1\left(\frac{Sc}{Pr_h}\right)_b g^*_{e\xi b} + \frac{5}{3}N_2 Sc_b\theta_0 T^*_{eb}g^*_{e\xi b} - \frac{5}{3}\frac{J\theta_0 N_{2b}}{C_b}\right] \quad (32)$$

where

$$Re_x = \frac{\rho_\infty^2 U_\infty^2 x^2}{s} = \frac{\rho_\infty^2 U_\infty^2 x}{(\rho_\infty \eta_\infty U_\infty)_{\text{aver.}}}$$

$$(\rho\ \eta\ U\ )_{\text{aver.}} = \frac{1}{x}\int_0^\psi \rho\ \eta\ U\ \mathrm{d}x \quad (33)$$

$$J = \frac{j_e k_B}{e}\frac{m_e\sqrt{2s}}{R^*\rho_\infty\eta_\infty U_\infty g_{e0}}.$$

For the stagnation point heat transfer, the following relation is valid:

$$Nu_D = -\frac{q_b D_0}{k_{hb}T_{h0}} = \sqrt{(2K)}\left(\frac{\rho_b}{\rho_\infty}\right)\sqrt{(Re_D)}\left[T^*_{h\xi b} + N_1\left(\frac{Sc}{Pr_h}\right)_b g^*_{e\xi b} + \frac{5}{3}N_2 Sc_b\theta_0 T^*_{eb}g^*_{e\xi b} - \frac{5}{3}\frac{J\theta_0 N_{2b}}{C_b}\right] \quad (34)$$

where

$$Re_D = \frac{\rho_\infty U_0 D_0}{\eta_\infty},$$

$$J = \frac{j_e k_B m_e\sqrt{2}}{eR^* g_{e0}\sqrt{(\rho_\infty\eta_\infty K U_0/D_0)}} \quad (35)$$

$K = 2$ or 3 for cylinder or sphere, respectively.

E. *Boundary-layer thicknesses and potential drop*

The following quantities are sometimes useful for comparison of boundary-layer flows:

(1) *Displacement thickness.*

$$\delta^* = \int_0^\infty\left(1 - \frac{\rho u}{\rho_\infty U_\infty}\right)\mathrm{d}y = \frac{\sqrt{2s}}{\rho_\infty U_\infty r_0^k}\int_0^\infty \frac{\rho_\infty}{\rho}\left(1 - \frac{\rho}{\rho_\infty}f_\xi\right)\mathrm{d}\xi. \quad (36)$$

(2) *Momentum thickness.*

$$\delta_m = \int_0^\infty \frac{\rho u}{\rho_\infty U_\infty}\left(1 - \frac{u}{u_\infty}\right) dy = \frac{\sqrt{2s}}{\rho_\infty U_\infty r_0^k} \int_0^\infty f_\xi(1 - f_\xi)\, d\xi. \quad (37)$$

(3) *Resistive potential drop.*

$$\varphi = \int_0^\infty \left(\frac{j_e}{\sigma} - \frac{j_e}{\sigma_\infty}\right) dy = \frac{j_e}{\sigma_\infty}\frac{\sqrt{2s}}{\rho_\infty U_\infty r_0^k} \int_0^\infty \frac{\rho_\infty}{\rho}\left(\frac{\sigma_\infty}{\sigma} - 1\right) d\xi. \quad (38)$$

Because of the similarity in these expressions with the equation to compute y, equation (19) is

$$y = \frac{\sqrt{2s}}{\rho_\infty U_\infty r_0^k} \int_0^\xi \frac{\rho_\infty}{\rho}\, d\xi. \quad (39)$$

Equations (36)–(39) all have the common factor $\sqrt{2s}/\rho_\infty U_\infty r_0^k$. It can be shown that this factor when applied to planar and stagnation point flows, respectively, may be written as

$$\frac{\sqrt{2s}}{\rho_\infty U_\infty r_0^k} = \frac{x\sqrt{2}}{\sqrt{Re_x}}, \text{ or } \frac{D_0}{\sqrt{2KRe_D}}. \quad (40)$$

From equations (38) and (40) it can be shown that, as long as the temperatures in the free stream remain constant along the flow direction, for a given applied voltage, the current distribution is given by $j \propto x^{-0.5}$, and a locally similar solution is possible. It is, however, very unlikely that the temperature in the axial direction does remain constant because of the joule heating, and, consequently, the complication of the current distribution forces the search for a non-similar solution.

III. NUMERICAL COMPUTATIONS AND RESULTS FOR AN ARGON PLASMA

A. *Transport properties*

Solution of the differential equations, equations (20), (22), (24) and (26), given in the previous section for a real gas requires a knowledge of several thermophysical and transport properties. Even for a plasma in thermal equilibrium ($T_e = T_h$), one must rely mostly on the theoretical predictions of the transport properties. The two methods currently in use are the Fay mixture rule [20] and the theory by de Voto [21–23] which follows the Chapman–Enskog method [24].

Because the methods to compute the transport properties of a thermally non-equilibrium plasma [25–30] are too complicated to be of any practical use, some new methods to compute these are necessary. Therefore, a modification of the Fay mixing rule is taken. This rule has the advantage of indicating the role of the individual species contribution to the transport properties of the mixture. Several authors [7, 31] have discussed the applicability of using Fay's mixing rule.

Because the mean thermal velocity of the electrons is very large in comparison to the heavy particles (atoms a and ions i), the heavy particles appear to be almost static with respect to the electrons. Therefore, for binary electron encounters with heavy particles, the electron temperature is used to calculate the collision cross sections and the collision frequency. From the heat-conductivity coefficient for "pure" atoms and electrons, k'_a and k'_e, Fay's mixing rule, taking into consideration the heat-conductivity coefficient of a fully ionized plasma due to Spitzer, k_S, the relation for the total heat-conductivity coefficient is derived as follows:

$$k = \frac{x_e k_S/3}{3x_e + \sqrt{(2)}x_a \dfrac{Q_{ea}}{Q_{ee}}} + \frac{x_a k'_a}{x_a + \dfrac{x_e Q_{ai}}{Q_{aa}}}. \quad (41)$$

This value of k is considered to be equal to $(k_e + k_h)$ in the present notation [equation (7)]

when $T_e = T_h$. For this to be true, the first term on the right of equation (41), which applies for a fully ionized plasma, is assumed to apply for a partially ionized gas as well. Thus, the individual heat-conductivity coefficients become

$$k_e = \frac{x_e k_S/3}{3x_e + \sqrt{(2)}x_a \dfrac{Q_{ea}}{Q_{ee}}}, \quad k_h = \frac{x_a k'_a}{x_a + \dfrac{x_e Q_{ai}}{Q_{aa}}}. \tag{42}$$

Detailed equations to compute the transport properties are given in the Appendix.

B. *Reaction rates*

For an argon plasma, the following reactions are taken into consideration:

$$\left.\begin{aligned} a + a &\rightleftharpoons i + e + a \\ a + e &\rightleftharpoons i + e + e. \end{aligned}\right\} \tag{43}$$

Harwell and Jahn [32] considered reaction by direct ionization either in a single- or two-step mechanism involving an intermediate excited state a^*. They conclude from their experiments that the two-step mechanism is most important. By combining the forward reaction rate for low ionized plasma by Kelly [33] and the rate for strongly ionized plasma by Hinnov and Hirschberg [34] with the equilibrium condition, the following reaction rate for an argon plasma is derived:

$$\begin{aligned} R_e = R_i = -R_a \\ = n_a \cdot 2{\cdot}3638 \cdot 10^{-41} T_h^{3/2} \left[2 + \frac{1{\cdot}34 \cdot 10^5}{t_h}\right] \\ \times \exp\left(-\frac{1{\cdot}34 \cdot 10^5}{T_h}\right) \cdot \left(n_a - \frac{n_e^2}{S(T_h)}\right) \\ + 5{\cdot}6 \cdot 10^{-33} \left(\frac{T_e}{11600}\right)^{-4{\cdot}5} \\ \times S(T_e) n_e \left(n_a - \frac{n_e^2}{S(T_e)}\right), \quad \mathrm{m^{-3}s^{-1}}. \end{aligned} \tag{44}$$

The value S is the Saha function given by

$$S = \left(\frac{n_e^2}{n_a}\right)_{\text{eq.}} = \frac{2Z_i}{Z_a}\left(\frac{2\pi M_e k_B}{h^2}\right) T_e \exp\left(-\frac{I_i}{kT_e}\right). \tag{45}$$

The second part of equation (44) was found to be consistent with results given by Park [35] and Bates [36]. The reaction rate computed from equation (44) is used to compute the mass rate of production m_R.

Exact solution of the differential equations [equations (20), (22), (24) and (26)] with the boundary conditions of equation (29) is extremely difficult because of the strongly interacting and non-linear behavior of the differential equations. The non-similar source terms resulting from current flow and collisional energy exchange are very important terms which introduce instabilities in solving the differential equations. The exact magnitude of the collisional energy exchange term is not known, and it is usual to introduce an energy loss factor δ_c, which is multiplied with the collisional energy exchange term. Demetriades [37] investigated the energy loss factors for elastic and inelastic collisions between electrons and heavy particles. He found that the energy loss factor for inelastic collisions which results from the transfer of the energy of the excited particle to the incoming electron is relatively small and can be neglected. The effective electron energy loss factor for all processes and species is in fact usually very small compared to unity [37]. Camac and Kemp [11] attempted to solve the differential equations without any current flow and found possible solutions only if the energy loss factor $\delta_c = 0$ or if $\delta_c \to \infty$. The present results apply for $\delta_c = 1$.

C. *Method of solution*

Before describing the present method, it may be pointed out that several other numerical methods were attempted without much success. These include, for instance, the method of perturbation of the initial boundary conditions to match the final boundary conditions [38] and a shooting-technique by laying a band on final boundary conditions [10].

Since it is not possible to obtain a complete locally similar solution for all differential equations, local similarity is imposed on the momentum equation only, equation (20). This means

that all partial derivatives of f with respect to s are zero. The validity of a local similarity is, however, not shown.

The general form of the other differential equations is

$$fF_\xi + (AF_\xi)_\xi + 2sS = 2s(f_\xi F_s - f_s F_\xi) = 2sf_\xi F_s. \quad (46)$$

From the value of the properties at ∞, $S_\infty = F_{s\infty}$ and, assuming $F_s(\xi) = F_{s\infty}$, equation (46) is simplified to

$$fF_\xi + (AF_\xi)_\xi + 2s(S - f_\xi S_\infty) = 0. \quad (47)$$

Several authors have given approximate methods [39, 40] to solve the laminar boundary-layer equations for a low-temperature, non-current carrying gas. Solutions with and without current flow are obtained in the present case using a simpler approximate series of the following type together with the boundary conditions of equation (29):

$$F = a_1 + a_2\xi + a_3 \exp(-\xi) + a_4 \exp(-2\xi). \quad (48)$$

Numerical computations were done for an argon plasma at $p = 10^{-2}$–1 bar, $T_{e0} = 10\,000$–$16\,000$°K, $T_{h0} = 6000$–$16\,000$°K, and $|j_e| < 10^6$ A/m^2 with $T_{e\infty}$ increased not more than 1·1 T_{e0}.

For no suction or blowing ($f_w = 0$) and without a pressure gradient ($\beta = 0$), the value of $(f_{\xi\xi})_b$ obtained by the present method was found to be somewhat higher than the more exact results of Back [41] (0·62 instead of his value of 0·47). Back's analysis does not take into account an applied electric field. At larger values of β, the present results tend to increase much faster than do those of Back. These comparisons with Back's analysis can be made since the momentum equations in both cases are identical. It was also found that at $\rho_\infty/\rho_w \ll 1$, $f_{\xi\xi}$ is almost independent of β.

From the free-fall edge analysis with current flow, it was found that $g^*_{eb} \approx 0$ and that

$$T^*_{eb} = T^*_{e\infty}, \quad T^*_{h\xi_b} = 0{\cdot}602\text{–}0{\cdot}650, \quad g^*_{e\xi_e} = 0{\cdot}664. \quad (49)$$

For moderate current densities ($|j_e| < 10^6$ A/m^2), the gradients are independent of the current density and depend mainly on the temperatures in the free stream. Thus the analysis applies for current densities adjacent to the anode that do not exceed about 10^6 A/m^2 which occurs at lower pressures or to a situation of plasma flowing over a biased wall. It is, therefore, possible to compare the gradients with the more accurate analyses of other authors [6, 11] who did not allow for current flow. The relationships for the gradients obtained from these other authors are:

$$T^*_{h\xi_b} = 0{\cdot}47\, C_b^{0{\cdot}1}\alpha(T_{h\infty}), \quad C = \frac{\rho\eta}{\rho_\infty\eta_\infty} \quad (50)$$

$$g^*_{e\xi_b} = 0{\cdot}47\,\frac{C_b^{0{\cdot}1}}{Sc_b^{\frac{1}{3}}}, \quad Sc = \frac{\rho D_{\text{amb}}}{\eta}. \quad (50a)$$

For a constant Prandtl number, it has been found [10] that $\alpha \propto Pr^{\frac{1}{3}}$, but for an argon plasma [6], $\alpha = 0{\cdot}4$–1 for $T_{h\infty} < 20\,000$°K, $p = 1$ bar. For an argon plasma at $T_{e0} = T_{h0} = 12\,000$°K and $p = 1$ bar, equations (50) and (50a) were evaluated taking the following computed values: $C_b = 29{\cdot}0$, $Sc_b = 0{\cdot}369$ and $\alpha = 0{\cdot}42$. The resulting values of the gradients are: $T^*_{h\xi_b} = 0{\cdot}2764$ and $g^*_{e\xi_b} = 0{\cdot}918$. The discrepancies between these values and those obtained by the present analysis given in equation (49) occur because for the series solutions of the energy and species continuity equations, only two exponential terms were used in equation (48). Since in equations (24) and (26), the source terms are much smaller than the convective terms and can be neglected, the resulting equations are identical to those for no-current, equal-temperature ($T_e = T_h$) plasmas which were solved by several authors [6, 11]. The same terms, however, dominate in the electron energy equation (25), and cannot be neglected. It is, therefore, recommended to use the more exact values of $g^*_{e\xi}$ and $T^*_{h\xi}$ from other authors given by equations (50) and (50a) for the evaluation of convective and diffusive heat transfer and to use the present analysis to evaluate the heat transfer caused by the current.

D. *Heat transfer, boundary-layer thicknesses and potential drop*

Since the gradients of equations (50) and (50a) are believed to give more accurate results of the convective and diffusive heat transfer, it is recommended that these equations be combined with equations (32) and (34) to evaluate the Nusselt number. The third term in the bracket on the right side in equations (32) and (34), however, contributes less than five per cent of the second term and has been dropped. With this limitation, the following Nusselt number relations are derived from which the total heat transfer may be computed for planar and stagnation point flow, respectively:

$$Nu_x = -\frac{q_b x}{k_{hb} T_{h0}} = \left(\frac{\rho_b}{\rho_\infty}\right) \sqrt{(Re_x)}\, C_b^{0.1} \times \left[0{\cdot}332 \left\{\alpha + N_1 \left(\frac{Sc^{\frac{1}{3}}}{Pr_h}\right)_b\right\} - 1{\cdot}1785 \frac{J\theta_0 N_{2b}}{C_b^{1.1}}\right] \quad (51)$$

and

$$Nu_D = -\frac{q_b D_0}{k_{hb} T_{h0}} = 2\sqrt{(k)} \left(\frac{\rho_b}{\rho_\infty}\right) \sqrt{(Re_D)}\, C_b^{0.1} \left[0{\cdot}332 \times \left\{\alpha + N_1 \left(\frac{Sc^{\frac{1}{3}}}{Pr_h}\right)_b\right\} - 1{\cdot}1785 \frac{J\theta_0 N_{2b}}{C_b^{1.1}}\right]. \quad (52)$$

The dimensionless numbers are defined by equations (33) and (35). To determine the importance of the individual terms in equations (51) and (52), the following computed values for an argon plasma at $p = 1$ bar, $T_{e0} = T_{h0} = 12\,000$°K are taken: $Sc_b = 0{\cdot}369$, $N_1 = 1{\cdot}23$, $N_{2b} = 0{\cdot}0484$ and $\alpha = 0{\cdot}42$. N_1 is not very sensitive to the temperature of the heavy particles, but is extremely sensitive to the pressure and the electron temperature. Since the term α and $(Sc^{\frac{1}{3}}/Pr_h)_b$ in equations (51) and (52) pertain to the convective and diffusive energy transfer, it is evident that the diffusive energy transfer is significant for the above plasma condition. At a low ionization fraction of the plasma, however, the diffusive transfer mechanism can be neglected. Experimental results of Massier *et al.* [42] show that for no-current flow in a low temperature plasma ($T_h \approx T_e < 8000$°K and low-ionization fraction) at $p \approx 0{\cdot}3$ bar, the release of ionization energy by recombination of diffusing particles to the surface is not very important. Other authors [43, 44] measured heat fluxes on probes placed between two electrodes. Because in those cases, the current was flowing parallel to the surface, no direct comparison is possible. It can, however, be shown that at high temperature, the recombination of the diffusing particles may have a very significant effect. Petrie and Pfender [44] found, at $p = 1$ bar, that the heat flux is from 1 to 2 orders of magnitude larger than is expected without considering diffusion.

The last term in brackets [ ] in equations (51) and (52) pertains to the energy transfer carried by the current. It is this term that represents the major effort of the present analysis. The effect of the current flow on the overall heat flux can be shown by simplifying the product (JN_{2b}) by first defining a length based on equations (25) and (31) as follows:

$$L_c = 0{\cdot}471 \left[\frac{e}{(\eta_b k_B)}\right] \left(\frac{k_{hb}}{j_e}\right). \quad (53)$$

After substituting equation (53) into equation (30) and writing the relations for gradients from equations (50) and (50a), the Nusselt number for configurations in general becomes

$$Nu_L = \left(\frac{\rho_b}{\rho_\infty}\right) \left[0{\cdot}332\, C_b^{0.1} \sqrt{(Re_L)} \left\{\alpha + N_1 \times \left(\frac{Sc^{\frac{1}{3}}}{Pr_h}\right)_b + 0{\cdot}5553\, N_{2b} Sc_b^{\frac{1}{3}} \theta_0\right\} - \frac{1{\cdot}1785\, \theta_0}{C_b^{0.1}} \frac{L}{L_c}\right]. \quad (54)$$

Equation (54) can be applied to the plane and

stagnation point flows by making the appropriate substitutions as was done previously, namely:

For plane flow.

$$L = x, \quad Re_L = Re_x = \frac{\rho_\infty^2 U_\infty^2 x^2}{s}.$$

For stagnation point flow.

$$L = D_0, \quad Re_L = 4KRe_D = \frac{4K\rho_0 U_0 D_0}{\eta_0}. \quad (55)$$

From equations (8) and (55), one can then write for the local heat flux

$$q = -\frac{Nu_L k_{hb}}{L} = -\frac{A_1}{L} + j_e(A_2 + \varphi_A + \phi_w). \quad (56)$$

By comparing equations (56) with (54), (53) and (31), the coefficient A_1 represents

$$A_1 = \frac{\rho_b U_0 r_0^k k_{hb} T_{h0}}{0{\cdot}1}\, 0{\cdot}332\, C_b^{0{\cdot}1}\left\{\alpha + N_1 \times \left(\frac{Sc^{\frac{1}{3}}}{Pr_h}\right)_b + 0{\cdot}5553\, N_{2b} Sc_b^{\frac{1}{3}}\theta_0\right\}$$

and the coefficient A_2 represents

$$A_2 = 2{\cdot}5021\, \frac{\rho_b}{\rho_\infty}\, \frac{\theta_0 T_{h0}\eta_b k_B}{C_b^{0{\cdot}1} e}. \quad (57)$$

These coefficients are computed separately for a particular gas and at a particular state. For a typical argon plasma flowing over a flat copper anode at $p = 1$ bar, $T_{e0} = T_{h0} = T_{e\infty} = T_{h\infty} = 12\,000$°K, $T_w = 400$°K and $U_0 = 10$ m/s with values of φ_A and ϕ_w for copper of 2 V and 4·3 V respectively, the heat flux becomes

$$q = -\frac{0{\cdot}65}{x^{0{\cdot}5}} + 6{\cdot}8 j_e, \quad \text{kW/cm}^2. \quad (58)$$

In equation (57), the value of x is in cm and j_e is in kA/cm^2 (thousands of A/cm^2). A comparison of the relative significance of the two terms in equation (58) becomes evident in the following example. At $x = 1$ m, $|j_e| = 10^6$ A/m^2, equation (58) gives the heat flux $q = 0{\cdot}745$ kW/cm^2, where the first term in the right side of equation (57) contributes only 10 per cent of the second term. At $x = 0{\cdot}25$ m, the contribution of the first term increases to only 20 per cent of the second term.

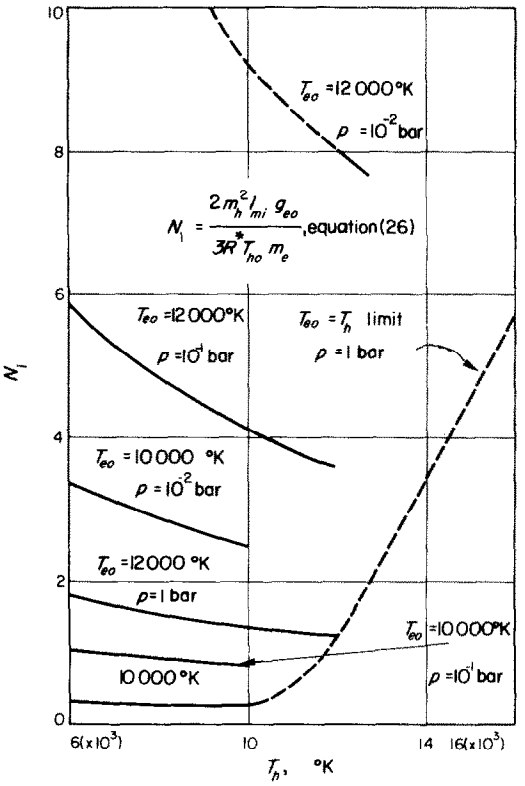

FIG. 3. Results for N_1 vs. T_h for argon.

The dimensionless numbers, N_1 and N_{2b}, for an argon plasma are plotted in Figs. 3 and 4. The Schmidt number Sc_b is in the range 0·35–0·38. It is evident that, at certain temperatures and low pressures, the term representing the diffusion of charged particles and recombination can contribute significantly to the total heat transfer.

Figures 5 and 6 show the profiles of thermophysical properties for argon plasma at $p = 1$ bar as a function of ξ. Figure 7 shows separately the state of the gas as dependent on the natural coordinate also. For comparison, Fig. 7 also contains equilibrium values of g_e.

For a typical condition of $p = 1$ bar, $T_{e\infty} = T_{h\infty} = 12\,000$°K, the following characteristic

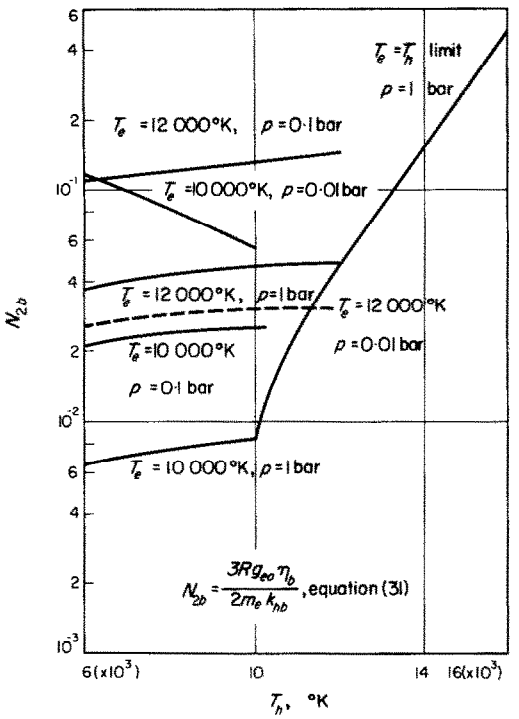

FIG. 4. Results for N_2 vs. T_h for argon.

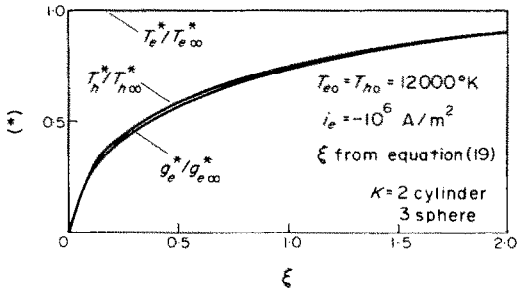

FIG. 5. Profiles for g_e, T_e, T_h in transformed coordinates.

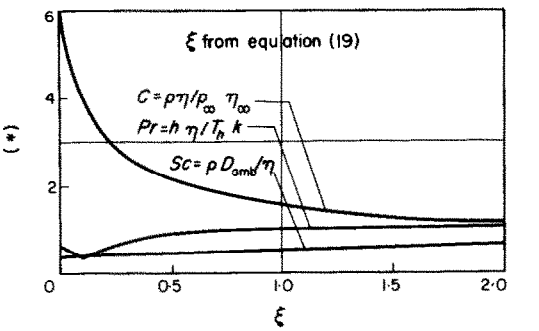

FIG. 6. Profiles for C, Prandtl and Schmidt numbers.

boundary-layer thicknesses and resistive potential drop are computed for plane and stagnation point flows, respectively.

$$\left.\begin{aligned}\delta^* &= \left(\frac{x}{\sqrt{Re_x}} \text{ or } \frac{D_0}{2\sqrt{KRe_D}}\right) \times 0{\cdot}05630\\ \delta_m &= \left(\frac{x}{\sqrt{R^2{}_x}} \text{ or } \frac{D_0}{2\sqrt{KRe_D}}\right) \times 0{\cdot}773\\ \varphi &= -\left(\frac{x}{\sqrt{Re_x}} \text{ or } \frac{D_0}{2\sqrt{KRe_D}}\right)\frac{j_e}{\sigma_\infty} \times 1{\cdot}51544\end{aligned}\right\} \quad (59)$$

For comparison with a constant-properties gas on a plane plate [45], $\delta^* = 1{\cdot}72x/\sqrt{Re_x}$, and $\delta_m = 0{\cdot}664x/\sqrt{Re_x}$. Note that as a consequence of the small density ratio ρ_∞/ρ, which results from the high gas temperature of 12 000°K, the coefficient for δ^* is very small in comparison to the constant properties gas, but the coefficient for δ_m is not very sensitive to the density ratio as may be seen by examining equation (37).

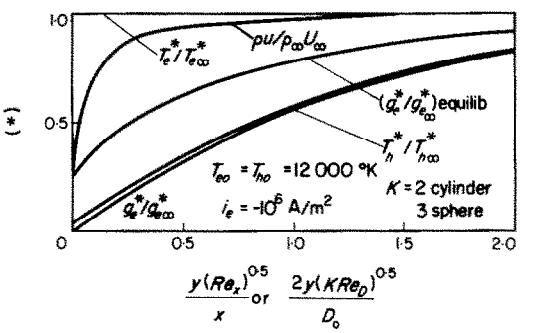

FIG. 7. Profiles for g_e, T_e, T_h and mass flux in natural coordinates.

IV. SUMMARY AND CONCLUSIONS

A theoretical study has been presented of heat transfer from a two-temperature argon plasma in the presence of an electric field applied perpendicular to the surface of a body. The analysis may be applied to plasma flow over flat-plate electrodes or axisymmetric bodies when the

approaching flow has been pre-ionized. In the presence of an electric field, the electrons acquire energy which is transformed into random thermal energy by collisions; however, they remain at an elevated temperature because of conditions for which there are an insufficient number of collisions with heavy particles to equilibrate the temperatures. The heat-transfer relations were derived in terms of Nusselt number which has been based on the assumption that the wall temperature is negligibly small compared to the gas temperature. Relations for argon flow in configurations in general and for flow over a flat plate as well as flow in the stagnation region of an axisymmetric body are given by equations (54), (51) and (52), respectively. More general heat-transfer equations, (30), (32) and (34), were also derived which may be used for other gases. They were obtained from an approximate solution of the laminar boundary-layer equations by matching the conditions at the outer edge of the free-fall region, b, and at the free-stream edge of the boundary layer, $\xi \to \infty$. The values of the layer distributions are, however, not exact between the free-fall region b and the free-stream edge of the boundary layer ($\xi > 0$). Because the objective of the study was primarily to evaluate the heat flux, this approach is considered to give satisfactory results. Therefore, the boundary-layer distributions shown in Figs. 5–7 normalized with values at $\xi \to \infty$ are exact only at the two boundaries.

Numerical calculations were made for flow over flat-plate electrodes for conditions in which the electron and heavy particles temperatures increased as much as 10 per cent above the temperatures of the approaching flow. It was found that, for the maximum current density for which the analysis applies ($j_e < 10^6$ A/m^2) and for 10 per cent increase in free-stream temperatures, the profiles of $f_\xi = u/U_\infty$, $T_e/T_{e\infty}$, and $T_h/T_{h\infty}$ are insensitive to current, although $T_{e\infty}$ and $T_{h\infty}$ may change along the flow. Furthermore, the convective heat flux is dependent on the temperature gradient of the heavy particles at the wall and includes a contribution due to enthalpy transport by the electrons. The temperature gradient of the heavy particles at the free-fall edge b, however, is independent of the current density. The results show that the effect of an elevated electron temperature is negligible on convective and diffusive heat transfer, but is significant for the overall heat transfer due to energy transport by the current. The contribution of the heat flux to the anode by the current includes the increase in energy gained by the electrons in the anode fall region and the "condensation" of the electrons at the surface (work function). In general, the total heat flux to the anode is computed from equation (8); however, equation (8) includes a radiation term which is not evaluated in this analysis. For argon specifically, the total heat flux may be computed by using a combination of equations (56) and (57). An example is given for specific flow conditions.

ACKNOWLEDGEMENT

The financial support of this program by NASA, through the National Research Council, Washington, D.C., is gratefully acknowledged.

REFERENCES

1. J. L. KERREBROCK, Conduction in gases with elevated electron temperature. *Engineering Aspects of Magnetohydrodynamics*, pp. 327–246. Columbia University Press (1962).
2. W. D. HAYES, On laminar boundary layers with heat transfer, *Jet Propulsion* **26**, 270–274 (1956).
3. J. G. SKIFSTAD and S. N. B. Murthy, Analysis of arc-heating phenomena in a tube, *IEEE Trans. Nucl. Sci.* **92** (1964).
4. A. SHERMAN and E. RESHOTKO, The nonequilibrium boundary layer along a channel wall, *AIAA 6th Aerospace Sciences Meeting*, New York, AIAA Paper 68-134, 1968; also Non-equilibrium boundary layer along an insulator wall, *AIAA Jl* **7**, 610–615 (1969).
5. W. L. BADE, Stagnation point heat transfer in a high-temperature inert gas, *Physics Fluids* **5**, 150–154 (1962).
6. T. K. BOSE, Der Waermeuebergang von Argon- und Stickstoff-plasma an eine kalte Wand, Dissertation, Tech. Univ., Stuttgart, Germany (1965); also in *Proc. Energy Conversion, Electric Propulsion and Plasma Flows*, DLR-67-17, Stuttgart (October 1967).
7. L. H. BACK, Laminar boundary layer heat transfer from a partially ionized monatomic gas by similarity approach, Technical Report 32-867, Jet Propulsion Laboratory, Pasadena, California (February 1966); also, *Physics Fluids* **10**, 807–819 (1967).
8. H. MIRELS and W. E. WELSH, JR., Stagnation point

boundary layer with large wall to free stream enthalpy ratio, *AIAA Jl* **6**, 1105–1110 (1968).
9. H. Mirels, Subsonic flow of hot gas through a highly cooled channel, *AIAA Jl* **6**, 1585–1587 (1968).
10. L. H. Back, Effects of severe surface cooling and heating on the structure of low-speed, laminar boundary layer gas flows with constant free-stream velocity, ASME Paper, no. 68-HT-23 (August 1968).
11. M. Camac and N. H. Kemp, A multi-temperature boundary layer, *AIAA Conference on Physics of Entry into Planetary Atmospheres*, Cambridge, Massachusetts, AIAA Paper 63-460 (26–28 August 1963).
12. T. K. Bose, Laminar flow heat transfer of gas plasma at elevated electron temperature in presence of electromagnetic fields, Technical Report 32-1447, Jet Propulsion Laboratory, Pasadena, California (March 1970).
13. K. T. Shih, E. Pfender, W. E. Ibele and E. R. G. Eckert, Experimental studies of the electrode heat transfer in an MPD arc configuration, *AIAA Electric Propulsion and Plasma Dynamics Conference*, Colorado Springs, Colorado, AIAA Paper 67-673 (1967).
14. K. T. Shih, E. Pfender, W. E. Ibele and E. R. G. Eckert, Experimental anode heat transfer studies in a co-axial arc configuration, *AIAA Jl* **6**, 1482–1487 (1968).
15. T. K. Bose, Experimental and theoretical studies on electrostatic probes, Heat Transfer Lab., Univ. of Minnesota, Minn., HTL-TR-83 (May 1968).
16. J. O. Hirschfelder, C. F. Curtiss and R. B. Bird, *Molecular Theory of Gases and Liquids*. John Wiley (1954).
17. A. Unsöld, *Physik der Sternatmosphören*. Springer Verlag (1955).
18. J. Grey and P. F. Jacobs, Cooled electrostatic probe, *AIAA Jl* **5**, 84–90 (1967).
19. L. Lees, Laminar heat transfer over blunt-nosed bodies at hypersonic flight-speeds, *Jet Propulsion* **26**, 259–269 (1956).
20. J. A. Fay, Hypersonic heat transfer in air boundary layer, *High Temperature Aspects of Hypersonic Flow*, edited by W. C. Nelson, pp. 583–605. McMillan (1964).
21. R. S. de Voto, Transport properties of ionized gases, *Physics Fluids* **9**, 1230–1240 (1966).
22. R. S. de Voto, Transport coefficients of partially ionized argon, *Physics Fluids*, **10**, 354–364 (1967).
23. R. S. de Voto, Simplified expressions for the transport properties of ionized monatomic gases, *Physics Fluids* **10**, 2105–2112 (1967).
24. S. Chapman and T. G. Cowling, *The Mathematical Theory of Non-uniformed Gases*. London (1953).
25. K. Harstad, Transport equations for gases and plasmas by the 13-moment method: a summary, Technical Report 32-1318, Jet Propulsion Laboratory, Pasadena, Calif. (October 1968); also, private communication.
26. D. M. Dix, Energy transfer processes in a partially ionized, two-temperature gas, *AIAA Jl* **2**, 2081–2090 (1964).
27. V. S. Galkin, Application of the Chapman–Enskog method to the case of a two-temperature binary gas mixture, *Akad. Nauk SSSR, Izv. Mekh. Zhid. Gaza* (in Russian), 58–63 (November–December 1967).
28. R. M. Chmieleski and J. H. Ferziger, Transport properties of a non-equilibrium partially ionized gas, *Physics Fluids* **10**, 364–371 (1967).
29. C. H. Kruger and M. Mitchner, Kinetic theory of two-temperature plasmas, *Physics Fluids* **10**, 1953–1961 (1967).
30. N. Jhunjhunwala and D. Mintzer, Equilibration of a uniform two-temperature mixture of Maxwell molecules, *Physics Fluids* **11**, 1300–1307 (1968).
31. A. B. Witte, Experimental investigation of an arc-heated supersonic free jet, Part I of Ph.D. Thesis, California Institute of Technology, Pasadena, California (May 1967).
32. E. Harwell and A. G. Jahn, Ionized rates in shock-heated argon, krypton, and xenon, *Physics Fluids* 7, 214–222 (1964).
33. A. J. Kelly, Atom–atom ionization cross sections of the noble gases—argon, krypton, and xenon. *J. Chem. Phys.* **45**, 1723–1732 (1966).
34. E. Hinnov and J. G. Hirschberg, Electron ion recombination in dense plasmas, *Phys. Rev.* **124**, 795 (1962).
35. C. Park, Measurement of ionic recombination rate of nitrogen, *AIAA Jl* **6**, 2090–2094 (1968).
36. D. R. Bates, A. E. Kingston and R. W. P. McWhirter, Recombination between electrons and atomic ions. I. Optically thin plasmas, *Proc. R. Soc.* **267A**, 297–312 (1962).
37. S. T. Demetriades, Determination of energy-loss factors for slow electrons in hot gases, *Phys. Rev.* **158**, 215–217 (1967).
38. F. Dewey, Jr. and J. F. Gross, Exact similar solutions of the boundary-layer equations. *Advances in Heat Transfer*, Vol. 4. Academic Press (1967).
39. S. Levy and R. A. Seban, Skin friction and heat transfer for laminar boundary layer flow with variable properties and variable free-stream velocity, *J. Appl. Mech.* **75**, 415–421 (1953). Comments by W. B. Brown, E. R. G. Eckert and J. N. B. Livingwood, *J. Appl. Mech.* **76**, 89–90 (1954).
40. L. Devan, Approximate solution of the compressible laminar boundary-layer equations, *AIAA Jl* **6**, 2010–2012 (1968).
41. L. H. Back and A. B. Witte, Prediction of heat transfer from laminar boundary layers, with emphasis on large free-stream velocity gradients and highly cooled walls, *J. Heat Transfer* **88C**, 249–256 (1966).
42. P. F. Massier, L. H. Back and E. J. Roschke, Heat transfer and laminar boundary-layer distributions in an internal subsonic gas stream at temperatures up to 13, 900°R, *J. Heat Transfer* **91C**. 83–90 (1969).
43. W. Springe, Waermeuebergang an ein gekuehltes Rohr im Lichtbogen Plasma, Ph.D. Thesis, Tech. University, Braunschweig, Germany (1960).
44. T. W. Petrie and E. Pfender, Heat-transfer studies to a wire probe immersed in an arc plasma, ASME Paper 68-HT-49 (June 1968).
45. E. R. G. Eckert and R. M. Drake, *Heat and Mass Transfer in a Monatomic Gas*. McGraw-Hill (1959).
46. A. B. Cambel, *Plasma Physics and Magnetofluid Dynamics*. McGraw-Hill (1963).

47. J. A. FAY and N. H. KEMP. Theory of end heat transfer in a monatomic gas, including ionization effects. Report 166, AVCO-Everett Research Lab. (March 1963).
48. T. K. BOSE. Experimental and theoretical studies on electrostatic probes. Report HTL-TR-83. Heat Transfer Lab., University of Minnesota, Minneapolis, Minnesota (May 1968).
49. G. W. SUTTON and A. SHERMAN. *Engineering Magnetohydrodynamics*. McGraw-Hill (1965).

APPENDIX

Thermophysical Transport Properties for a Singly-Ionized Plasma

Given T_e, T_h, p, the composition for an equilibrium plasma is computed as follows:

(1) *Saha function.*

$$S = \frac{n_i n_e}{n_a} = \frac{2Z_i}{Z_a}\left(\frac{2\pi m_e k_B}{h^2}\right)^{1.5} T_e^{1.5} \exp\left(-\frac{I_i}{k_B T_e}\right), \quad \mathrm{m}^{-3}$$

I_i = ionization potential, eV.

(2) *Temperature ratio.*

$$\theta = \frac{T_e}{T_h}.$$

(3) *Number densities.*

$$n_e = n_i = 0{\cdot}5\left[-S(\theta+1) + \left\{S^2(\theta+1)^2 + \frac{4pS}{k_B T_h}\right\}^{0.5}\right], \quad \mathrm{m}^{-3}$$

$$n_a = \left(\frac{p}{k_B T_h}\right) - n_e(\theta+1), \quad \mathrm{m}^{-3}.$$

Given T_e, T_h, p, g_e, the composition for a quasi-neutral plasma is computed as follows:

(1) *Temperature ratio.*

$$\theta = \frac{T_e}{T_h}.$$

(2) *Mass density.*

$$\rho = \frac{p m_h}{[R^* T_h (1 + \theta (m_h/m_e) g_e)]}$$

(3) *Number densities.*

$$g_i = \frac{m_i}{m_e} g_e, \quad g_a = 1 - g_i$$

$$\rho_j = \rho g_j$$

$$n_j = \frac{R^*}{k_B m_j}\rho_j.$$

Given T_e, T_h, n_j, the thermophysical and transport properties are computed, as follows:

(1) *Cross sections* [46–48].

$$Q_{jk} = f(T_e, T_h), \quad \mathrm{m}^{-2}.$$

(2) *Mol ratio*

$$x_j = \frac{n_j}{\sum n_j}$$

(3) *Ionization fraction*

$$\alpha_i = \frac{n_e}{n_a + n_e}$$

(4) *Viscosity coefficient of pure substance.*

$$\eta_j = 8{\cdot}38587 \times 10^{-26}\frac{(T_j m_j)^{0.5}}{Q_{jj}}, \quad \frac{\mathrm{kg}}{\mathrm{ms}}.$$

(5) *Thermal conductivity coefficient of pure substance.*

$$k'_j = 6{\cdot}24895 \times 10^{-22} \times 4{\cdot}187\frac{(T_j m_j)^{0.5}}{Q_{jj}}, \quad \frac{J}{\mathrm{ms^\circ K}}.$$

(6) *Thermal conductivity for electrons (Spitzer's equation* [20, 31]).

$$k'_S = \frac{4{\cdot}4 \times 4{\cdot}187 \times 10^{-11} T_e^{2.5}}{\log_e(1{\cdot}24 \times 10^7 T_e^{1.5}/n_e^{0.5})}.$$

(7) *Fay's mixing rule for viscosity coefficient* [20, 31].

$$\eta = \frac{\eta_a}{1 + \dfrac{\alpha_i Q_{ia}}{(1-\alpha_i)Q_{aa}}} + \frac{\eta_i \alpha_i}{\alpha + \dfrac{\eta_i Q_{ia}}{\eta_a Q_{aa}}(1-\alpha_i)}, \quad \frac{\mathrm{kg}}{\mathrm{ms}}.$$

(8) *Fay's mixing rule for thermal conductivity coefficient* [20, 31].

$$k = k_h + k_e, \quad \frac{J}{\mathrm{ms^\circ K}}$$

$$k_h = \frac{x_a k'_a}{x_a + \left(\dfrac{x_e Q_{ai}}{Q_{aa}}\right)}, \quad k_e = \frac{x_e k'_S/3}{3x_e + \sqrt{2}x_a\left(\dfrac{Q_{ea}}{Q_{ee}}\right)}.$$

(9) *Binary diffusion coefficients* [49].

$$D_{jk} = 42{\cdot}69375\frac{\left(\dfrac{T_j}{m_j} + \dfrac{T_k}{m_k}\right)^{0.5}}{(n_j + n_k)Q_{jk}}, \quad \frac{\mathrm{m}^2}{\mathrm{s}}.$$

(10) *Ambipolar diffusion coefficients* [49].

$$D_{amb} = \frac{2D_{ea}D_{ei}}{(D_{ea} + D_{ei})}.$$

(11) *Electrical conductivity for slightly ionized plasma (Chapman–Cowling)* [46].

$$\sigma_c = \frac{e^2 n_e D_{ea}}{k_B T_e}, \quad \frac{A}{Vm}.$$

(12) *Electrical conductivity for fully ionized plasma (Spitzer–Härm)* [46].

$$\sigma_S = \frac{1{\cdot}56 \times 10^{-2} T_e^{1{\cdot}5}}{\log_e \left(\frac{1{\cdot}24 \times 10^7 T_e^{1{\cdot}5}}{n_e^{0{\cdot}5}} \right)}. \quad \frac{A}{Vm}.$$

(13) *Electrical conductivity for arbitrary ionized plasma* [46].

$$\sigma = \frac{\sigma_c \times \sigma_S}{\sigma_c + \sigma_S}.$$

(14) *Collision frequency of electron-heavy particle collision.*

$$\Gamma_{eh} = c_e (n_a Q_{ae} + n_i Q_{ie})_{ne}, \quad m^{-3}s^{-1}$$

$$c_e = \left(\frac{8k_B T_e}{\pi m_e} \right)^{0.5}.$$

TRANSFERT THERMIQUE ANODIQUE POUR UN ÉCOULEMENT DE PLASMA D'ARGON À TEMPÉRATURE ÉLECTRONIQUE ÉLEVÉE

Résumé—On étudie théoriquement le transfert thermique depuis un plasma de gaz pré-ionisé s'écoulant sur une surface anodique à une température électronique élevée et en présence d'un champ électrique normal à la surface. On considère une couche limite laminaire dans laquelle seul le profil de vitesse est localement similaire et où les propriétés du fluide sont supposées changer uniformément dans la direction de l'écoulement gazeux. Les résultats obtenus par une méthode d'approximation montrent que pour des densités de courant modérées $|j_e| < 10^6$ A/m^2, les distributions de vitesse et de température sont insensibles au courant. De plus, l'effet de température électronique élevée sur le transfert thermique convectif est négligeable, mais il est sensible pour le transfert thermique global dû au transport d'enthalpie par le courant. Le flux thermique total à l'anode est obtenu par l'évaluation du nombre de Nusselt et par adjonction de termes dus à la chute de potentiel dans l'enveloppe et à la fonction de travail superficiel.

WÄRMEÜBERGANG AUF DIE ANODE BEI EINEM STRÖMENDEN ARGON-PLASMA MIT ERHÖHTER ELEKTRONENTEMPERATUR

Zusammenfassung—Theoretisch wird der Wärmeübergang von einem vor-ionisierten gasförmigen Plasma, das über die Anodenfläche strömt, bei erhöhter Elektronentemperatur in Abwesenheit eines elektrischen Feldes, das normal zur Oberfläche steht, untersucht. Es wird eine laminare Grenzschicht betrachtet, wobei nur das Geschwindigkeitsprofil lokal ähnlich ist und von den Flüssigkeitseigenschaften angenommen wird, dass sie sich in der Strömungsrichtung des Gases monoton ändern. Die durch die Näherungsmethode erhalten Ergebnisse zeigen, dass für mässige Stromstärken $|j_e| < 10^6$ A/m^2 die Geschwindigkeits-und Temperaturverteilungen unabhängig vom Strom sind. Der Einfluss erhöhter Elektronentemperatur ist für den konvektiven Wärmeübergang vernachlässigbar, aber wesentlich für den gesamten Wärmeübergang wegen des Enthalpietransportes im Strom. Den gesamten Wärmestrom erhält man durch die Terme für den Potentialabfall in der Hülle und die Oberflächenarbeitsfunktion.

ТЕПЛООБМЕН АНОДА ПРИ ТЕЧЕНИИ ПЛАЗМЫ АРГОНА ПРИ ПОВЫШЕННОЙ ТЕМПЕРАТУРЕ

Аннотация—Проводится теоретическое исследование переноса тепла от предварительно ионизированной газовой плазмы, обтекающей поверхность анода при повышенной электронной температуре и при наличии электрического поля, перпендикулярного поверхности. Рассмотрен ламинарный пограничный слой, в котором профили скорости подобны только локально, и принимается, что свойства жидкости равномерно изменяются в направлении течения газа. Полученные результаты показывают, что для умеренных плотностей тока $|Je| < 10^6$ А/м^2 ток не оказывает влияния на распределение скорости и температуры. Кроме того, влиянием повышенной электронной температуры на конвективный теплообмен можно пренебречь, однако это влияние существенно для общего теплообмена благодарч переносу энтальпии током. Суммарный тепловой поток к аноду получается из расчета числа Нуссельта и сложения членов, обязанных падению потенциала в электронной оболочке с функцией работы.